EFFECTS OF TANGENTIAL EDGE CONSTRAINTS ON THE POSTBUCKLING BEHAVIOR OF FLAT AND CURVED PANELS SUBJECTED TO THERMAL AND MECHANICAL LOADS

by

L. Librescu and W. Lin
Virginia Polytechnic Institute and State University
Blacksburg, Virginia

and

M. P. Nemeth and J. H. Starnes, Jr.
NASA Langley Research Center
Hampton, Virginia

Presented at the Symposium on Buckling and Postbuckling of Composite Structures

ASME Winter Meeting

November 6-11, 1994
Chicago, Illinois

EFFECTS OF TANGENTIAL EDGE CONSTRAINTS ON THE POSTBUCKLING BEHAVIOR OF FLAT AND CURVED PANELS SUBJECTED TO THERMAL AND MECHANICAL LOADS

L. Librescu and W. Lin
Virginia Polytechnic Institute and State University
Blacksburg, Virginia

M. P. Nemeth and J. H. Starnes, Jr.
NASA Langley Research Center
Hampton, Virginia

ABSTRACT

A parametric study of the effects of tangential edge constraints on the postbuckling response of flat and shallow curved panels subjected to thermal and mechanical loads is presented. The mechanical loads investigated are uniform compressive edge loads and transverse lateral pressure. The temperature fields considered are associated with spatially nonuniform heating over the panels, and a linear through-the-thickness temperature gradient. The structural model is based on a higher-order transverse-shear-deformation theory of shallow shells that incorporates the effects of geometric nonlinearites, initial geometric imperfections, and tangential edge motion constraints. Results are presented for three-layer sandwich panels made from transversely isotropic materials. Simply supported panels are considered in which the tangential motion of the unloaded edges is either unrestrained, partially restrained, or fully restrained. These results focus on the effects of the tangential edge restraint on the postbuckling response. The results of this study indicate that tangentially restraining the edges of a curved panel can make the panel insensitive to initial geometric imperfections in some cases.

INTRODUCTION

Major portions of the structure of high-speed aerospace vehicles consist of flat and curved panels that are used as primary load carrying components. Some typical applications of these panels are aircraft stabilizers and fuselage sections and missile nose and body sections. Often, the preliminary design of these panels is based on the simplification that the edges are simply supported and that the supports are completely rigid. In practice, however, the supports are not completely rigid and they can deform elastically, especially in the tangential direction perpendicular to the panel edges. A tangential direction, as used herein, is intended to mean the direction of the unit outward normal to a panel edge in the plane tangent to the panel surface at any point on the panel edge. Thus, understanding the effects of tangential edge constraints on the postbuckling behavior of flat and curved panels is an important consideration in the design of these panels.

The present paper addresses the effects of tangential edge restraints on the postbuckling behavior of three-layer flat and shallow curved sandwich panels made of transversely isotropic materials and subjected to combined thermal and mechanical loads. The panels have uniform thickness and are balanced and symmetric laminates. The mechanical loads include both lateral pressure and uniform edge compression loads and the thermal loads include both spatially nonuniform temperature fields and linear through-the-thickness temperature gradients. A special purpose analysis that is well-suited for parametric studies is described that includes the effects of initial geometric imperfections and transverse-shear deformation. Results obtained using the analysis are presented for simply supported panels that show the effects of thermal loads, lateral pressure, and edge compression loads on their postbuckling characteristics for the full range of tangential edge restraints including elastic edge restraints.

ANALYSIS DESCRIPTION

The analysis used in the present study is based on a higher-order transverse-shear-deformation theory (HSDT) that includes the effects of geometric nonlinearities and initial geometric imperfections. The details of the theory are lengthy and only a summary of the analysis and some of the details concerning the tangential edge constraints are presented in the present paper. Details of the analysis are given in Ref. 1.

Thermoelastic Constitutive Relations

The thermoelastic constitutive equations used for the present study are for symmetrically laminated shallow curved panels with uniform thickness. The material is assumed to have thermoelastic transversely isotropic properties, with the plane of isotropy coinciding with the tangent plane at each point of the shell reference surface. The transversely isotropic constitutive equations are characterized by five elastic constants and two thermal coefficients. The elastic constants and thermal coefficients that characterize the plane of isotropy of the material are the elastic modulus E, Poisson's ratio ν, and thermal compliance λ. In addition, the elastic modulus E', Poisson's ratio ν', shear modulus G', and thermal compliance λ' characterize the material behavior perpendicular to the plane of isotropy. The coefficients of thermal expansion α and α' are related to the thermal compliances λ and λ' by equations presented in Refs. 1 and 2. For transversely isotropic materials the transverse thermal expansion coefficient α' is often much larger than the tangential coefficient α. In addition, the transformed reduced thermoelastic constitutive equations used in the higher-order transverse-shear-deformation theory indicate that the thermal compliances depend on the ratio of the elastic moduli E/E'. The corresponding equations based on classical shell theory do not have this dependence. Another important characteristic of transversely isotropic materials is that the transformed reduced thermal compliances can have negative values for ordinary values of E/E' and λ/λ' (see Refs. 1 and 2). These thermal compliances are always positive-valued for a strictly isotropic material.

Nonlinear Boundary-Value Problem

In the present study, the nonlinear equations governing the postbuckling response of shallow curved panels are represented as an extension of the classical von Karman-Marguerre-Mushtari nonlinear shallow shell equations that include the effects of geometric imperfections and transverse shear deformations. An Airy stress function is used to eliminate the shell inplane force equilibrium equations. Consequently, the compatibility equation for the membrane strains is included as a primary field equation of the nonlinear boundary-value problem along with the remaining shell out-of-plane force equilibrium equation and the two moment equilibrium equations. A partially inverted form of the constitutive equations is introduced in which the membrane strains are expressed in terms of the Airy stress function and the transverse displacement, and the bending stress resultants and transverse shear stress resultants are expressed

in terms of the rotations and the transverse displacement. Substituting these special constitutive equations into the three remaining shell equilibrium equations and into the strain compatibility equation yields four coupled partial differential equations in terms of the stress function, the transverse displacement, and the two rotations. The equations are reduced further by expressing the rotations in terms of the transverse displacement and a potential function $\Gamma(x_1,x_2)$. Substituting the resulting expression into the out-of-plane force equilibrium equation yields an equation in terms of the stress function and transverse displacement, and substituting this equation into the moment equilibrium equations yields a single Helmholz-type boundary layer equation in Γ that is totally uncoupled from the other equations. In general, however, the boundary-value problem remains coupled through the five boundary conditions at each edge of the shell.

The boundary conditions considered in the present study are simply supported boundary conditions with varying degrees of tangential edge restraint. The tangential edge restraints act in the direction of the unit outward normal to the panel edge in the plane tangent to the panel at each point on a panel edge. For these boundary conditions, the transverse displacement at each edge, the bending stress resultant acting about the axis parallel to each edge, and the rotation about the axis normal to each edge (in the tangent plane) are all zero-valued. The degree of tangential edge restraint considered herein is bounded by the cases in which the tangential motion of the unloaded edges of a panel are either unrestrained or completely restrained, respectively, in the inplane direction perpendicular to the panel edge. For these two cases, the panel edges are referred to herein as moveable and immovable edges, respectively. All intermediate cases are referred to herein as partially moveable edges and include elastically restrained edge constraints.

For a moveable edge, zero-valued tangential stress resultants are specified at the edge. In contrast, for an immovable edge, the components of the tangential motion in the tangent plane that are normal and parallel to the edge are restrained and unrestrained, respectively. For this case, the shear stress resultant on the edge is specified as zero-valued, and the normal displacement in the tangent plane is specified as zero-valued in an average sense. To make this displacement zero-valued in an average sense, the normal displacement in the tangent plane is obtained in terms of the transverse displacement and stress function by using the corresponding strain-displacement relation and constitutive equations and then by integrating the resulting expression over the planform of the shell. Setting the resulting equation equal to zero yields a fictitious tangential stress resultant normal to the edge that makes the corresponding displacement zero-valued in an average sense.

The analytical procedure used for panels with opposite edges that are partially moveable is similar to the procedure previously described for panels with immovable edges. In particular, the average end-shortening displacement Δ_1 between edges $x_1 = 0$ and $x_1 = L_1$ (see Fig. 1 for the definition of the coordinate directions) is related to the corresponding compressive edge load N_{11} by

$$\Delta_1 c_1 = -N_{11} \tag{1a}$$

where c_1 is the average tangential stiffness in the x_1- direction on each opposite plate edge. Similarly, for the edges $x_2 = 0$ and $x_2 = L_2$

$$\Delta_2 c_2 = -N_{22} \tag{1b}$$

where c_2 is the average tangential stiffness in the x_2- direction on each opposite plate edge. The expressions for the end-shortening displacements are given by

$$\Delta_1 = \frac{-1}{L_1 L_2} \int_0^{L_1} \int_0^{L_2} u_{1,1}\, dx_2 dx_1 \tag{2a}$$

$$\Delta_2 = \frac{-1}{L_1 L_2} \int_0^{L_1} \int_0^{L_2} u_{2,2}\, dx_2 dx_1 \tag{2b}$$

where u_1 and u_2 are the displacements in the x_1 and x_2 directions, respectively, and a comma followed by a subscript denotes partial differentiation. The average compressive edge loads are given by

$$-N_{11} = \frac{1}{L_2} \int_0^{L_2} F_{,22}\Big|_{x_1 = 0,\, L_1} dx_2 \tag{3a}$$

$$-N_{22} = \frac{1}{L_1} \int_0^{L_1} F_{,11}\Big|_{x_2 = 0,\, L_2} dx_1 \tag{3b}$$

where F is the stress function (see Ref. 1) given by

$$F(x_1,x_2) = F_1(x_1,x_2) - \frac{1}{2}\left[(x_2)^2 N_{11} + (x_1)^2 N_{22}\right] \tag{4}$$

The partially restrained edge conditions are obtained by substituting Eqs. (2), (3), and (4) into Eq. (1); expressing the displacements u_1 and u_2 in terms of the transverse displacement and stress function by using the corresponding strain-displacement relation and constitutive equations; and then by solving for fictitious edges loads N_{11} and N_{22} that yield the desired tangential stiffness constraint on the edges.

Equations (1) indicate that values of $\Delta_1 = 0$ and $\Delta_2 = 0$ correspond to immovable edges at $x_1 = 0$ and L_1 and $x_2 = 0$ and L_2, respectively. These conditions are enforced by selecting $c_1 = \infty$ and $c_2 = \infty$, respectively. In addition, values of $c_1 = 0$ and $c_2 = 0$ correspond to moveable edges at $x_1 = 0$ and L_1 and $x_2 = 0$ and L_2, respectively. For these moveable edge conditions, $N_{11} = 0$ and $N_{22} = 0$.

To measure the degree of edge restraint in a convenient way, alternate tangential stiffness parameters λ_1 and λ_2 are introduced herein such that $\lambda_1 = 0$ and $\lambda_1 = 1$ correspond to moveable and immovable edges at $x_1 = 0$ and L_1, respectively. Similarly, $\lambda_2 = 0$ and $\lambda_2 = 1$ correspond to moveable and immovable edges at $x_2 = 0$ and L_2, respectively. Partially restrained edges at $x_1 = 0$ and L_1 and $x_2 = 0$ and L_2 are defined by $0 < \lambda_1 < 1$ and $0 < \lambda_2 < 1$, respectively. These alternate tangential stiffness parameters are given by

$$\lambda_1 = \frac{(\tilde{b} + \tilde{c})\, c_1}{1 + (\tilde{b} + \tilde{c})\, c_1} \tag{5a}$$

$$\lambda_2 = \frac{(\tilde{b} + \tilde{c})\, c_2}{1 + (\tilde{b} + \tilde{c})\, c_2} \tag{5b}$$

where $(\tilde{b} + \tilde{c})$ is the tangential stiffness quantity defined in Ref. 1.

For the simply supported boundary conditions described above, the nonlinear boundary-value problem is uncoupled with respect to the potential function Γ and the solution to the Helmholz-type boundary layer equation in Γ is $\Gamma = 0$. Thus, for shells with the simply supported boundary conditions described herein, the nonlinear boundary-value problem reduces to two partial differential equations in terms of the Airy stress function and the transverse deflection v_3. These two equations are referred to herein as the von Karman-type compatibility and transverse force equilibrium equations.

Solution of the Nonlinear Equations

The nonlinear boundary-value problem in the present study is solved using Galerkin's method. First, the transverse deflection v_3 is expressed in terms of functions that satisfy the simply supported boundary conditions

$$v_3(x_1,x_2) = w_{mn} \sin\lambda_m x_1 \sin\mu_n x_2 \tag{6a}$$

where $\lambda_m = m\pi/L_1$, $\mu_n = n\pi/L_2$, and w_{mn} are the modal amplitudes and L_1 and L_2 are the panel side lengths. Following the results presented in Ref. 3, the initial geometric imperfection $\overset{0}{v}_3$ is expressed as

$$\overset{0}{v}_3(x_1,x_2) = \overset{0}{w}_{mn} \sin\lambda_m x_1 \sin\mu_n x_2 \tag{6b}$$

where $\overset{0}{w}_{mn}$ are the modal amplitudes of the initial geometric imperfection shape. Similarly, the applied temperature and pressure fields are most generally represented by Navier-type double Fourier sine series. In the present study, the temperature and pressure fields are approximated by

$$\overset{0}{T}(x_1,x_2) = \overset{0}{T}_{mn} \sin\lambda_m x_1 \sin\mu_n x_2 \tag{6c}$$

$$\overset{1}{T}(x_1,x_2) = \overset{1}{T}_{mn} \sin\lambda_m x_1 \sin\mu_n x_2 \tag{6d}$$

$$p_3(x_1,x_2) = p_{mn} \sin\lambda_m x_1 \sin\mu_n x_2 \tag{6e}$$

where $\overset{0}{T}$ and $\overset{1}{T}$ enter the analysis through the constitutive equations and are expressed in terms of the temperatures at $x_3 = h/2$ and $-h/2$ (these temperatures are denoted by T_u and T_b, respectively) and are given by

$$\overset{0}{T} = \tfrac{1}{2}(T_u + T_b) \tag{7a}$$

$$\overset{1}{T} = \tfrac{1}{h}(T_u - T_b) \tag{7b}$$

The temperature field is given by

$$T(x_1,x_2,x_3) = \overset{0}{T}(x_1,x_2) + x_3 \overset{1}{T}(x_1,x_2) \tag{7c}$$

The displacement expansions are substituted into the von Karman-type compatibility equation and the Airy stress function is obtained by solving the resulting linear nonhomogeneous partial differential equation. The remaining nonlinear partial differential equation is the von Karman-type equilibrium equation and is converted into a set of nonlinear algebraic equations using

Galerkin's method. This procedure yields the following set of M x N nonlinear algebraic equations for each set of wave forms determined by the index pair (m,n)

$$
\begin{aligned}
&R_{rs}\, w_{rs} + p_{rs}\, B_{rs} - \Pi \hat{T}_{rs}\, C_{rs} \\
&+ P_1\left[w_{rs}, \overset{0}{w}_{rs}, \hat{L}_{11}, \hat{L}_{22}\right] + P_2\left[w_{rs}^2, \overset{0}{w}_{rs}\right] + \\
&P_3\left[w_{rs}^3, \overset{0}{w}_{rs}\right] + P_4\left[w_{rs}, \overset{0}{w}_{rs}, \overset{0}{\hat{T}}_{rs}, \hat{T}_{rs}\right] = 0
\end{aligned}
\tag{8}
$$

where the indices r and s are not summed and have the values r = 1, 2,..., M and s = 1, 2,..., N. In Eqs. (8), P_1 and P_4, P_2, and P_3 are linear, quadratic, and cubic polynomials of the unknown modal amplitudes w_{rs}, respectively. The coefficients B_{rs}, C_{rs}, and R_{rs} are constants that depend on the material and geometric properties of the shell and $\hat{L}_{11}$ and $\hat{L}_{22}$ are normalized forms of the tangential stress resultants representing the mechanical loads.

The equilibrium configurations for a given flat or curved panel are obtained by solving the nonlinear algebraic equations given by Eqs. (8) by using Newton's method. Every solution to Eqs. (8) represents a possible stable or unstable equilibrium configuration. The stability of each equilibrium configuration is determined by evaluating the second variation of the total potential energy of the panel. Expressing Eqs. (8) symbolically as $\mathbf{L}(w_{rs}) = \mathbf{0}$ the second variation of the total potential energy of the panel is obtained by computing the Jacobian of $\mathbf{L}$ with respect to w_{rs} and evaluating it for each equilibrium configuration that is a solution of Eqs. (8). The stable equilibrium configurations are given by those that make the Jacobian positive definite.

RESULTS AND DISCUSSION

The results presented in the present paper focus on the effects of tangential edge restraints on the postbuckling behavior of simply supported flat and curved panels. The panels considered have a square planform with dimensions $L_1 = L_2 = \ell$ and a uniform thickness h. Results for flat panels are presented in Figs. 1 through 4, and results for curved panels are presented in Figs. 5 through 13. In these figures, results are presented for varying degrees of tangential edge restraint on opposite edges including the limiting cases of moveable and immovable edges. The degree of tangential edge restraint is indicated in the figures by the values of the parameters λ_1 for the edges $x_1 = 0$ and ℓ, and by λ_2 for the edges $x_2 = 0$ and ℓ. A value of zero for either of these parameters corresponds to moveable edges and a value of one corresponds to immovable edges. Partially restrained edges at $x_1 = 0$ and ℓ and $x_2 = 0$ and ℓ are defined in the figures by $0 < \lambda_1 < 1$ and $0 < \lambda_2 < 1$, respectively. The thick solid and dashed lines shown in the figures corresponds to the limiting cases of moveable and immovable edges, respectively.

The panels considered herein consist of three layers of elastic transversely isotropic material. For all of the results presented herein, values of $\nu = 0.2$ and $\alpha = 1.15 \times 10^{-6}$ in/in/^{o}F were used for Poisson's ratio, and the coefficient of thermal expansion of each layer, respectively. In addition, a value of $\nu' = 0.2$ was used for the through-the-thickness Poisson's ratio. The face sheets of each sandwich panel are identical, and the core is twice as thick as a face sheet. Moreover, the elastic moduli and thermal compliance coefficients for the face sheets are constant nondimensional ratios with values of $(E'/E)_f = 5$, $(E/G')_f = 10$, and $(\lambda/\lambda')_f = 1.4286$, respectively. Similarly, the elastic moduli and thermal compliance coefficients for the core are constant nondimensional ratios with values of $(E'/E)_c = 2$, $(E/G')_c = 30$, and $(\lambda/\lambda')_c = 1.2143$, respectively.

The results are presented in the form of curves that relate the magnitude of the average middle surface temperature $\overset{0}{T}$ at the center of a panel to the central transverse deflection or the average end shortening as a function of the degree of tangential edge restraint, and in some cases a subcritical compressive edge load or transverse pressure load. The applied subcritical inplane compression loads N_{11} and N_{22}, and the applied transverse pressure load p_3 are represented in the figures by the following nondimensional parameters

$$\tilde{L}_{11} = \frac{N_{11}\ell^2}{\pi^4 D} \tag{9a}$$

$$\tilde{L}_{22} = \frac{N_{22}\ell^2}{\pi^4 D} \tag{9b}$$

$$p = \frac{p_3(\ell/2,\ell/2)\ \ell^4}{Dh} \tag{10}$$

where D is the isotropic bending stiffness of the panel given by

$$D = \frac{E h^3}{12(1-\nu^2)} \tag{11}$$

At buckling, the parameters $\tilde{L}_{11}$ and $\tilde{L}_{22}$ correspond to the well-known definitions of the bifurcation buckling coefficients for isotropic panels that are denoted herein by $(\tilde{L}_{11})_{cr}$ and $(\tilde{L}_{22})_{cr}$. For example, for the square flat panels with moveable simply supported edges considered herein, the buckling coefficient has a value of 4 for uniaxial compressive loading. Similarly, nondimensional central transverse deflection δ and corresponding imperfection amplitude δ_o are used in the figures and are given by

$$\delta = \frac{w_3(\ell/2,\ell/2)}{h} \tag{12}$$

$$\delta_o = \frac{\overset{0}{w}_3(\ell/2,\ell/2)}{h} \tag{13}$$

For all the results presented herein, the temperature field is specified to be sinusoidally distributed across each surface of the panels considered in this study (see Eq. (6)). Two through-the-thickness temperature distributions are considered in this study. One temperature distribution has the same temperature ($T_u = T_b$) on both panel surfaces, and the other temperature distribution has unequal temperatures ($T_u \neq T_b$) on the panel surfaces. For all results presented involving a through-the-thickness temperature gradient, a constant value of $T_b = 70^oF$ was used to obtain the results. Likewise, a value of the panel length-to-thickness ratio $\ell/h = 100$ was used to obtain the results.

Studies of the effects of uniform temperature increase ($T_u = T_b$) on several of the postbuckling equilibrium configurations of a typical flat panel considered herein were conducted. These results

indicate that the stable postbuckling equilibrium configurations correspond to shapes given by $m = n = 1$ in Eq. (6a). This trend was found to be true for the range of structural parameters considered herein. In all subsequent figures, the magnitude of the temperature distribution given by $\overset{0}{T}_{11}$ is denoted by $\overset{0}{T}$ in the figures for convenience.

Results for Flat Panels

The effects of a tangential edge restraint on the postbuckling behavior of flat panels subjected to a uniform through-the-thickness temperature increase ($T_u = T_b$) are show in Figs. 1 through 3. The results shown in Figs. 1 and 2 are for panels with moveable edges at $x_1 = 0$ and ℓ and with varying degrees of equal tangential edge restraint at $x_2 = 0$ and ℓ. The results shown in Fig. 3 are for panels with both pairs of opposite edges having varying degrees of equal tangential edge restraint. Each of the panels shown in these figures have perfectly flat prebuckling shapes, and buckle due to the spatially nonuniform heating applied to the panel top and bottom surfaces. Buckling occurs at the bifurcation points indicated on the figures by the filled circles.

The results presented in Figs. 1 and 2 for panels with one pair of opposite edges equally restrained indicate that the buckling temperature decreases as the degree of tangential edge restraint increases. The lowest and highest buckling temperatures are for the panels with immovable and moveable edges, respectively. This trend is due to the increase in compressive stress that results from increasing the tangential edge restraint. Comparing the results presented in Figs. 1 and 3 shows that this effect is amplified when both pairs of opposite edges are restrained. The results in Figs. 1 through 3 also show that the postbuckling stiffness increases in the deep postbuckling range ($\delta > 2.0$) as the degree of tangential edge restraint increases. This behavior is attributed to an increase in panel membrane stiffness as the degree of tangential edge restraint increases.

The effects of tangential edge restraint on the postbuckling behavior of flat panels subjected to a linear through-the-thickness temperature increase ($T_u \neq T_b$) are show in Fig. 4. The results in this figure are for panels with both pairs of opposite edges having varying degrees of equal tangential edge restraint. These panels begin deflecting out-of-plane at the onset of applying the thermal load due to the bending moments induced by the through-the-thickness thermal gradient and do not have a bifurcation buckling load. Comparing these results with the results in Fig. 3 shows that the effect of a tangential edge restraint is much smaller for panels subjected to a through-the-thickness temperature gradient than for corresponding panels subjected to a uniform temperature. In addition, the results show an increase in overall bending stiffness with an increasing degree of tangential edge restraint which is more pronounced in the initial stage of the postbuckling response for panels with a through-the-thickness temperature gradient than for panels with a uniform through-the-thickness temperature.

Results for Curved Panels

The effect of tangential edge restraints on the nonlinear behavior of cylindrical panels with $\ell / R_2 = 0.3$ and subjected to a uniform through-the-thickness temperature increase is shown in Fig. 5. The results in this figure are for geometrically perfect cylindrical panels with tangential edge restraints on the curved edges. The straight edges are moveable and loaded by a uniform compressive edge load that is 75% of the corresponding bifurcation buckling load; i.e., $\tilde{L}_{22} = 0.75\,(\tilde{L}_{22})_{cr}$. These results indicate a monotonic temperature-deflection behavior for the panels for the full range of tangential edge restraint. This monotonic behavior is a result of the deflections associated with the uniform heating of a curved panel that increase its curvature in a stable manner (i.e., the panel deflects away from its projected planform when it is heated). In

addition, the panels with immovable edges are shown to have larger deflections than the corresponding panels with moveable edges at a given value of the temperature. This behavior is a result of additional transverse deflections due to the additional compression load induced by restraining the curved edges of the panels.

The effects of a tangential edge restraint on the nonlinear behavior of very shallow cylindrical panels ($\ell / R_2 = 0.03$) subjected to a through-the-thickness temperature gradient are shown in Fig. 6. The results in this figure are for geometrically perfect cylindrical panels with the curved edges tangentially restrained. The straight edges are moveable and loaded by a uniform compressive edge load $\bar{L}_{22} = 0.75\,(\bar{L}_{22})_{cr}$. The results in Fig. 6 show that the response curves for these panels have a limit point for values of the tangential edge restraint parameter $\lambda_1 \leq 0.3$, and that the thermal limit load increases as the value of λ_1 increases. For $\lambda_1 = 0.34$, the panel response curve has a bifurcation point. For $\lambda_1 > 0.34$, the panel response curve is characteristic of a stable monotonic temperature-deflection response.

The effects of initial geometric imperfections on the response of the curved panels represented in Fig. 6 are shown in Figs. 7 and 8. The results in Figs. 7 and 8 are for curved panels with positive initial geometric imperfections with amplitudes of 0.1 and 0.2, respectively. A positive imperfection amplitude is inward. The panels with the smaller imperfection amplitude have similar behavioral trends as the corresponding perfect panels shown in Fig. 6. However, the results for the imperfect panels indicate that the effects of the tangential edge restraint are more pronounced than for the perfect panels and that there is a substantial reduction in the thermal limit load for a given value of λ_1. The limit points for the imperfect panels occur for much higher values of λ_1 than for the perfect panels. The imperfect panels shown in Fig. 7 have a bifurcation point for $\lambda_1 = 0.67$, and a monotonic nonlinear behavior for values of $\lambda_1 > 0.67$. These differences in behavior indicate that tangentially restraining the edges of a curved panel can make the panel insensitive to initial geometric imperfections in some cases.

The results in Figs. 7 and 8 indicate that increasing the geometric imperfection amplitude of the panels eliminates the bifurcation and monotonic nonlinear responses of the panels. Panels with the larger imperfection amplitude $\delta_o = 0.2$ have a limit point behavior for the most part and panels with immovable curved edges have the highest value of thermal limit load.

The effects of subcritical circumferential compressive edge loads on the response of the curved panels represented in Fig. 6 are shown in Figs. 9 and 10. These subcritical edge loads for Figs. 9 and 10 have values given by $\bar{L}_{22} = 0.5\,(\bar{L}_{22})_{cr}$ and $\bar{L}_{22} = 0$, respectively. These results, and the results in Fig. 6, show that the response trends are very sensitive to the presence and magnitude of the circumferential compressive edge loads. The results show that reducing the value of $\bar{L}_{22}$ significantly reduces the sensitivity of the response to the degree of tangential edge restraint except in the deep postbuckling range of behavior. Similarly, reducing the value of $\bar{L}_{22}$ significantly changes the response trends of the panels. Panels with $\bar{L}_{22} = 0.5\,(\bar{L}_{22})_{cr}$ have a limit point response for the most part. The panels with the immovable edges have the highest value of thermal limit load. In contrast, all panels with $\bar{L}_{22} = 0$ have monotonically increasing transverse deflections with increasing temperature.

The effects of a tangential edge restraint on the nonlinear behavior of shallow cylindrical panels ($\ell / R_2 = 0.1$) subjected to a through-the-thickness temperature gradient are shown in Figs. 11 and 12. The results in these figure are for geometrically perfect cylindrical panels with their straight edges tangentially restrained. The curved edges are moveable and loaded by a uniform compressive edge load given by $\bar{L}_{11} = 0.75\,(\bar{L}_{11})_{cr}$. These results, and the results in Fig. 6

suggest that panels with restrained straight edges and loaded curved edges generally have the same response trends as panels with restrained curved edges and loaded straight edges. The panels of Figs. 11 and 12 have a limit point response for values of the tangential edge restraint parameter $\lambda_2 \leq 0.1$. The highest value of the thermal limit load for these panels is for $\lambda_2 = 0.1$. For $\lambda_2 = 0.18$, the panels have a bifurcation buckling load and for $\lambda_2 > 0.18$, the panels have a monotonic temperature-deflection response.

The effects of tangential edge restraints on the nonlinear behavior of shallow cylindrical panels ($\ell / R_2 = 0.1$) subjected to a through-the-thickness temperature gradient are shown in Fig. 13. The results in the figure are for geometrically perfect panels with the straight edges tangentially restrained and with moveable curved edges. The panels are loaded by an external transverse pressure load p_3, given by Eq. (6e) with $m = n = 1$. The magnitude of the pressure load is given by $p = 2$ (see Eqn. 10). The results shown in Figs. 6, 11, and 13 indicate that the effects of the degree of tangential edge restraint on the nonlinear behavior is qualitatively the same for panels that are loaded by transverse pressure and by inplane compressive loads. Comparing the results in Figs. 11 and 13 indicates that the pressure-loaded panels appear to be slightly more sensitive to the degree of tangential edge restraint than the compression-loaded panels. For example, the pressure-loaded panel with moveable straight edges ($\lambda_2 = 0$) has monotonically increasing transverse deflections with no limit point with increasing temperature and the corresponding panel with compression loaded curved edges has a limit point. In addition, the pressure-loaded panels have a bifurcation point for $\lambda_2 = 0.8$ and the corresponding compression-loaded panels shown in Fig. 11 have a bifurcation point for $\lambda_2 = 0.18$.

CONCLUDING REMARKS

The results of a parametric study of the postbuckling behavior of flat and curved panels subjected to thermal and mechanical loads have been presented. The mechanical loads considered in the study are uniform compressive edge loads that are less than the panel buckling loads and transverse lateral pressure. The temperature fields considered are associated with spatially nonuniform heating over the panel surfaces and a linear through-the-thickness temperature gradient. The analytical model used in the study is based on a higher-order transverse-shear-deformation theory of shallow shells that incorporates the effects of geometric nonlinearites and initial geometric imperfections. Results are presented for simply supported three-layer sandwich panels made from a transversely isotropic material.

The results presented herein show that flat panels subjected to a uniform through-the-thickness temperature are generally more sensitive to the degree of tangential edge restraint than the corresponding panels subjected to a through-the-thickness temperature gradient. For the cylindrical panels considered herein, the results show that the degree of tangential edge restraint can significantly change the character of the nonlinear response and, in some cases, make a panel insensitive to initial geometric imperfections. The results also show that the effects of a tangential edge restraint are more pronounced for geometrically imperfect curved panels than for the corresponding perfect panels, and that the response is more sensitive to the degree of tangential edge restraint when compressive edge loads are applied.

ACKNOWLEDGMENT

The work reported herein was partially supported by NASA Grant NAG1-1300.

REFERENCES

1. Librescu, L., Lin, W., Nemeth, M. P., and Starnes, J. H., Jr., "Classical Versus Non-Classical Postbuckling Behavior of Laminated Composite Panels Under Complex Loading Conditions," AMD-Vol. 164, Non-Classical Problems of the Theory and Behavior of Structures Exposed to Complex Environmental Conditions, ASME, 1993, pp. 169-182.

2. Librescu, L., "Elasto-Statics and Kinetics of Anisotropic and Heterogeneous Shell-Type Structures," Noordhoff International Publishers, The Netherlands, Leyden, 1975.

3. Seide, P., "A Reexamination of Koiter's Theory of Initial Postbuckling Behavior and Imperfection Sensitivity of Structures," Thin Shell Structures: Theory, Experiment and Design," Y. C. Fung and E. E. Sechler, Eds., Prentice-Hall, 1974, pp. 59-80.

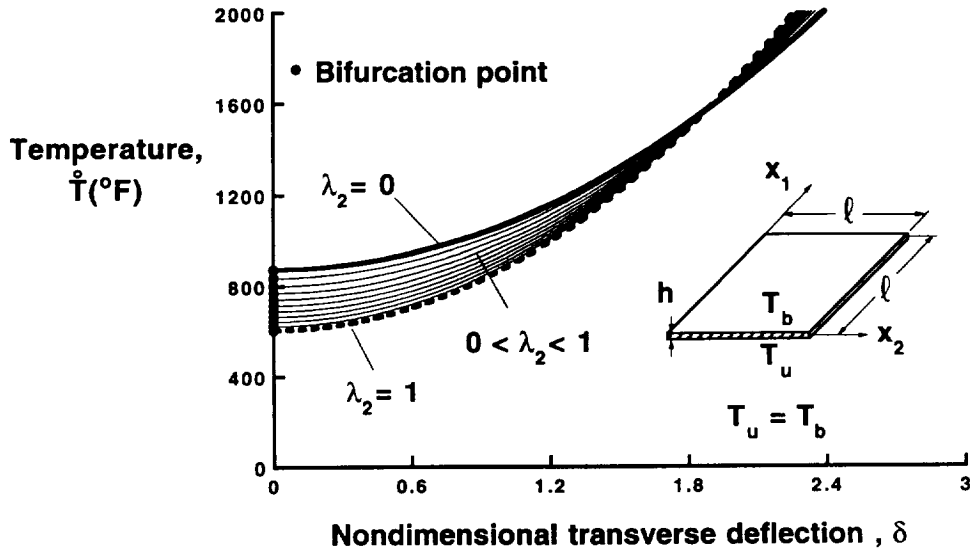

Fig. 1 Effects of tangentially restraining the panel edges at $x_2 = 0$ and $x_2 = \ell$ on the postbuckling response of flat panels (edges $x_1 = 0$ and $x_1 = \ell$ are moveable) subjected to uniform heating.

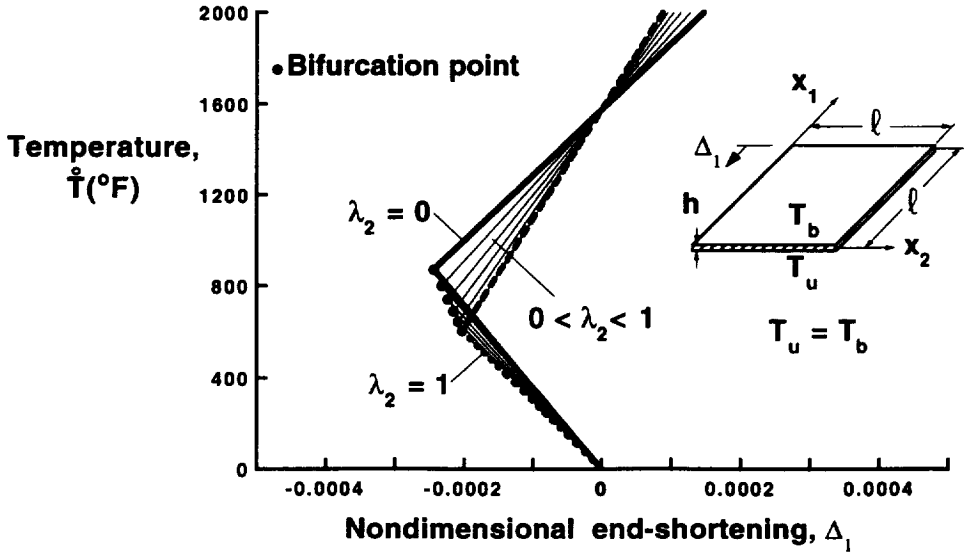

Fig. 2 Effects of tangentially restraining the panel edges at $x_2 = 0$ and $x_2 = \ell$ on the postbuckling response of flat panels (edges $x_1 = 0$ and $x_1 = \ell$ are moveable) subjected to uniform heating.

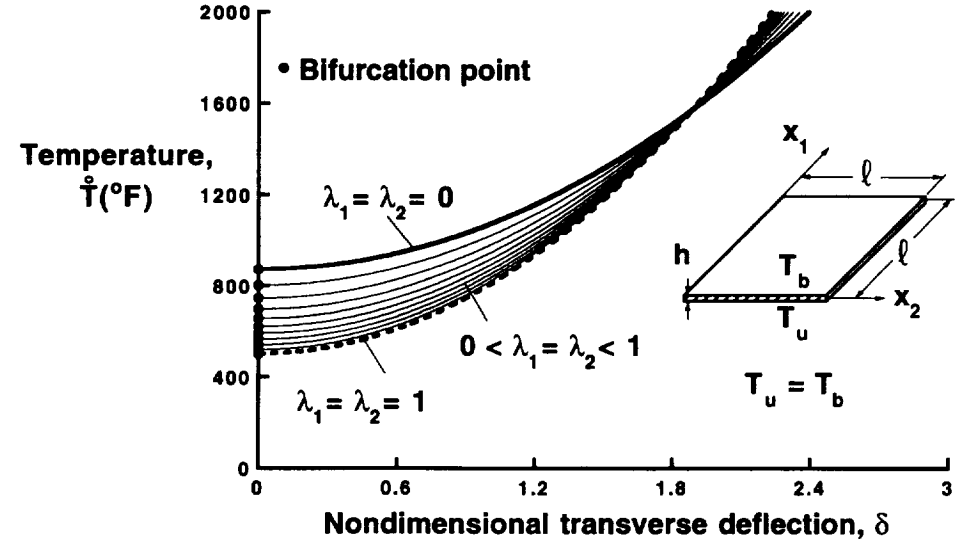

Fig. 3 Effects of tangentially restraining all panel edges on the postbuckling response of flat panels subjected to uniform heating.

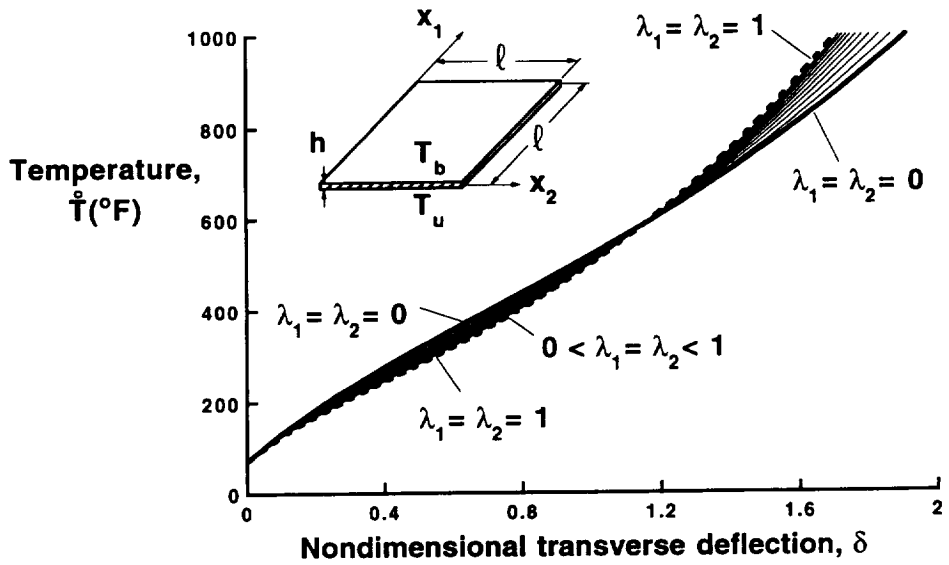

Fig. 4 Effects of tangentially restraining all panel edges on the postbuckling response of flat panels subjected to a through-the-thickness temperature gradient.

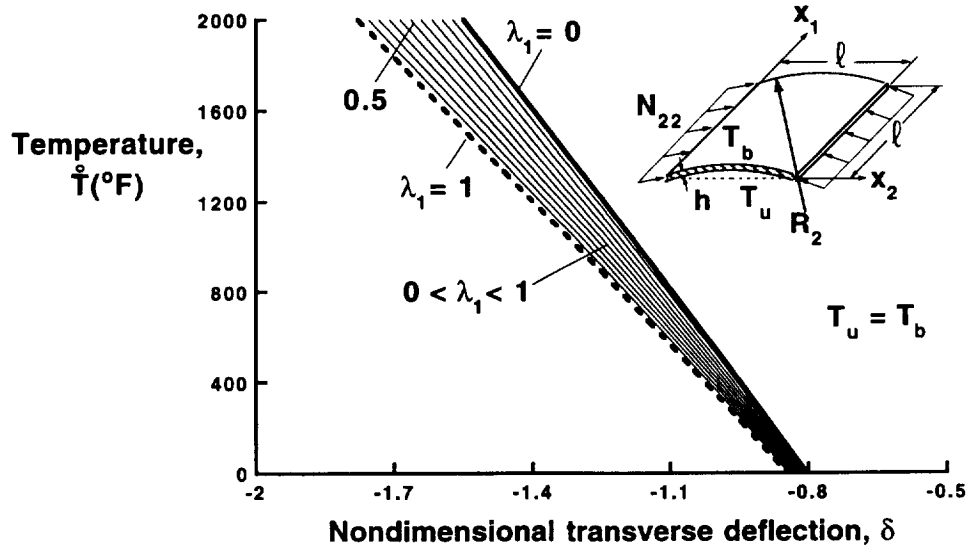

Fig. 5 Effects of tangentially restraining the curved edges on postbuckling response of cylindrical panels subjected to uniform heating and compressive edge loads ($\ell / R_2 = 0.3$, $\tilde{L}_{22} = 0.75 (\tilde{L}_{22})_{cr}$).

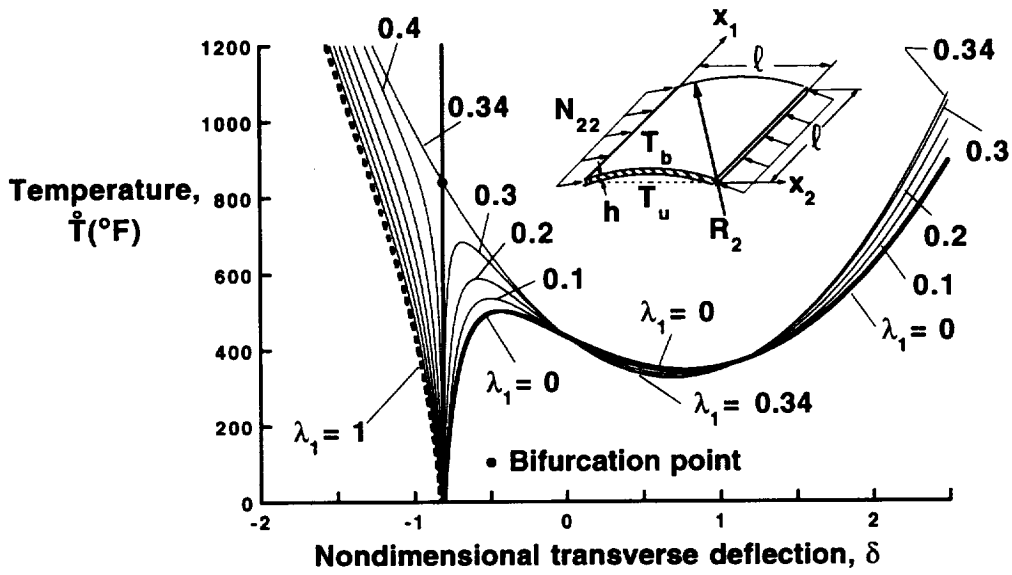

Fig. 6 Effects of tangentially restraining the curved edges on the postbuckling response of geometrically perfect cylindrical panels subjected to a through-the-thickness temperature gradient and a compressive edge load ($\ell / R_2 = 0.03$, $\tilde{L}_{22} = 0.75\,(\tilde{L}_{22})_{cr}$).

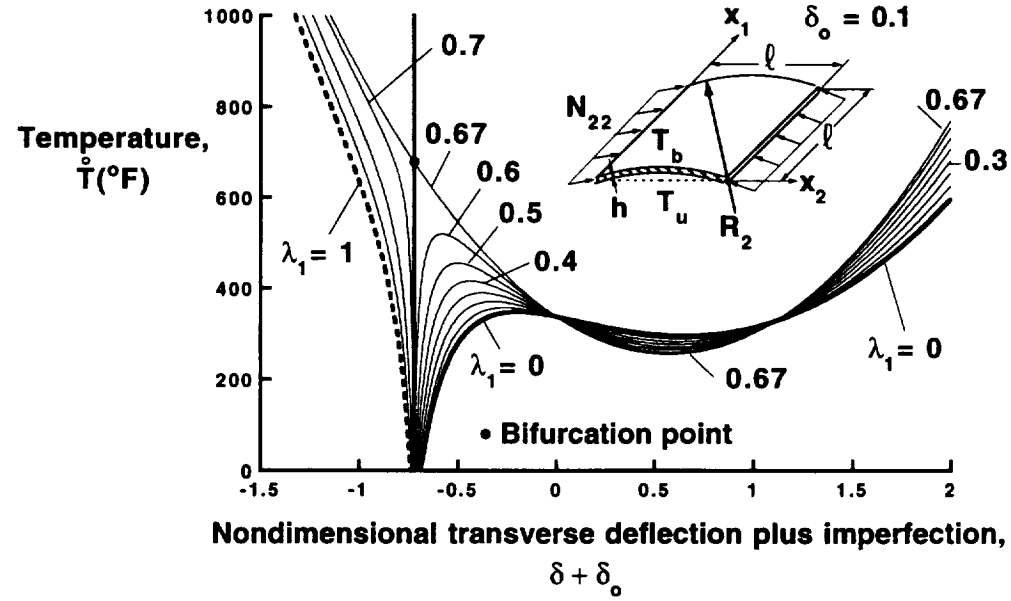

Fig. 7 Effects of tangentially restraining the curved edges on the postbuckling response of imperfect cylindrical panels subjected to a through-the-thickness temperature gradient and a compressive edge load ($\ell / R_2 = 0.03$, $\tilde{L}_{22} = 0.75\,(\tilde{L}_{22})_{cr}$, $\delta_o = 0.1$).

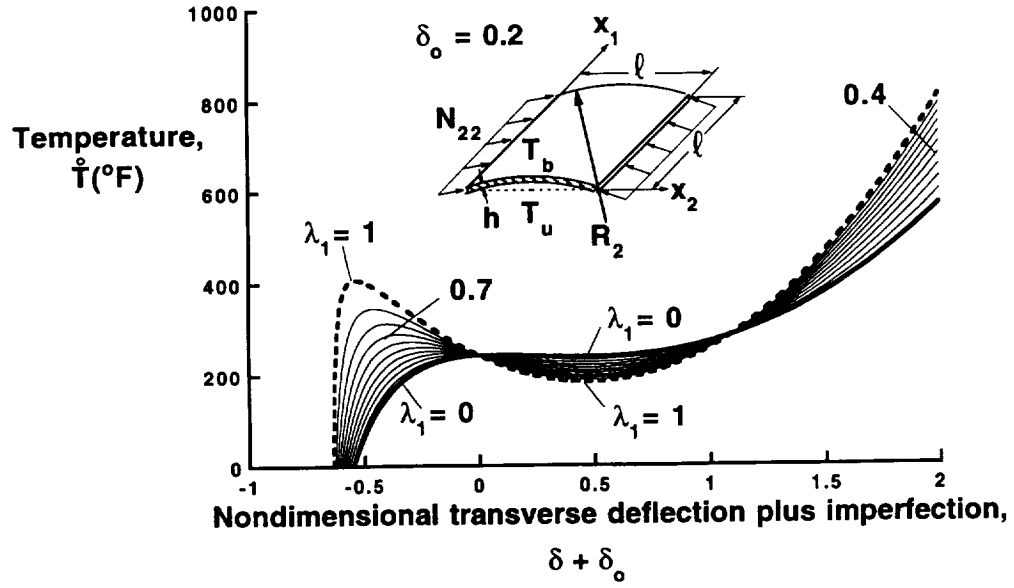

Fig. 8 Effects of tangentially restraining the curved edges on the postbuckling response of imperfect cylindrical panels subjected to a through-the-thickness temperature gradient and a compressive edge load ($\ell / R_2 = 0.03$, $\tilde{L}_{22} = 0.75 (\tilde{L}_{22})_{cr}$, $\delta_o = 0.2$).

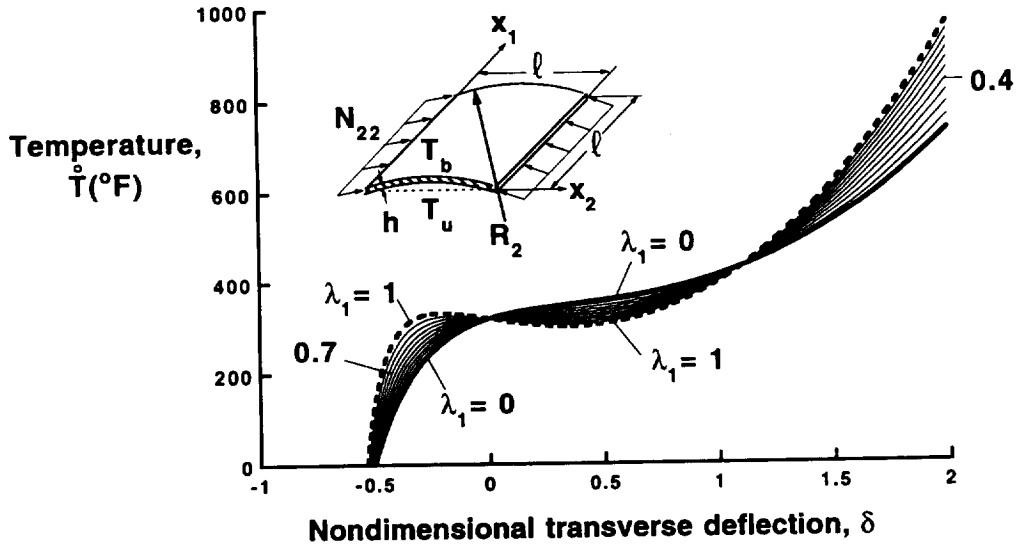

Fig. 9 Effects of tangentially restraining the curved edges on the postbuckling response of geometrically perfect cylindrical panels subjected to a through-the-thickness temperature gradient and a compressive edge load ($\ell / R_2 = 0.03$, $\tilde{L}_{22} = 0.5 (\tilde{L}_{22})_{cr}$).

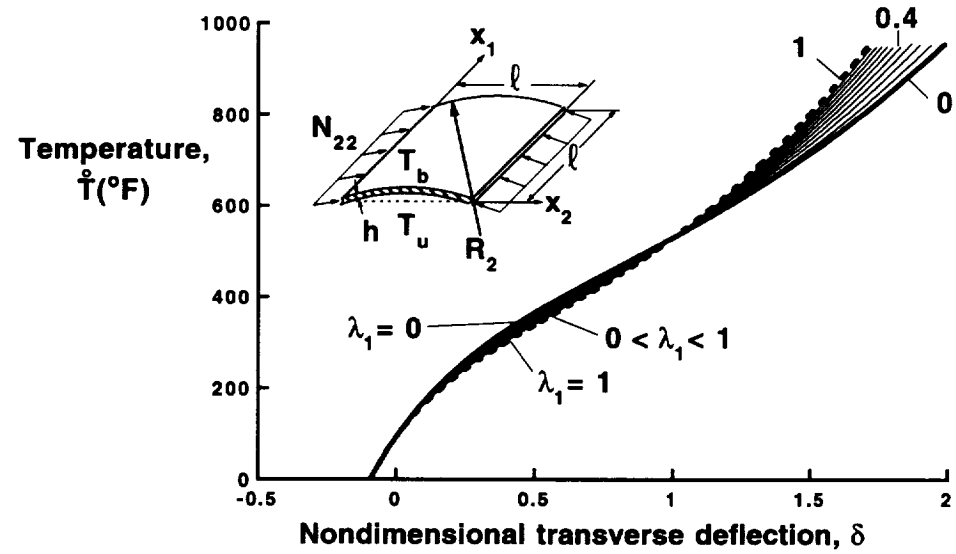

Fig. 10 Effects of tangentially restraining the curved edges on the postbuckling response of geometrically perfect cylindrical panels subjected to a through-the-thickness temperature gradient and a compressive edge load ($\ell / R_2 = 0.03$, $\tilde{L}_{22} = 0$).

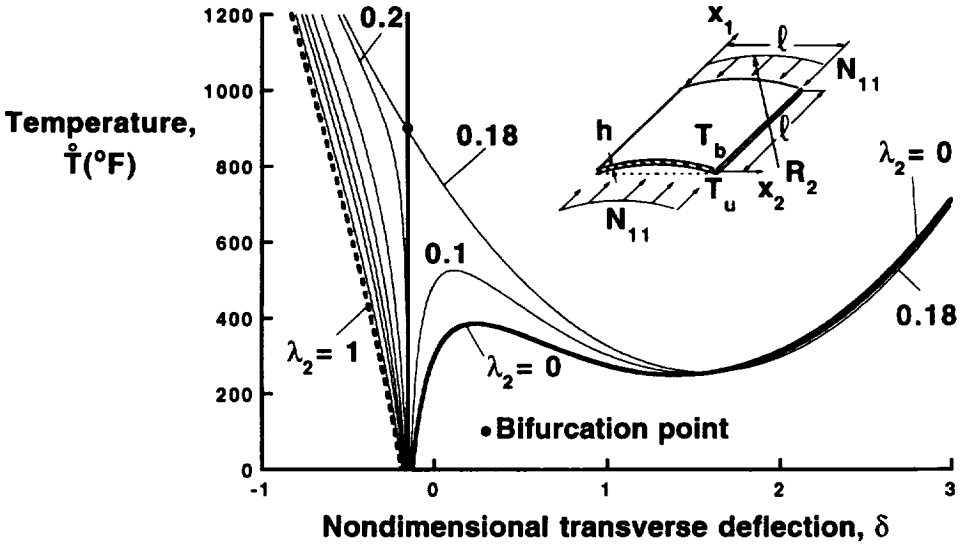

Fig. 11 Effects of tangentially restraining the straight edges on the postbuckling response of geometrically perfect cylindrical panels subjected to a through-the-thickness temperature gradient and a compressive edge load ($\ell / R_2 = 0.1$, $\tilde{L}_{11} = 0.75 (\tilde{L}_{11})_{cr}$).

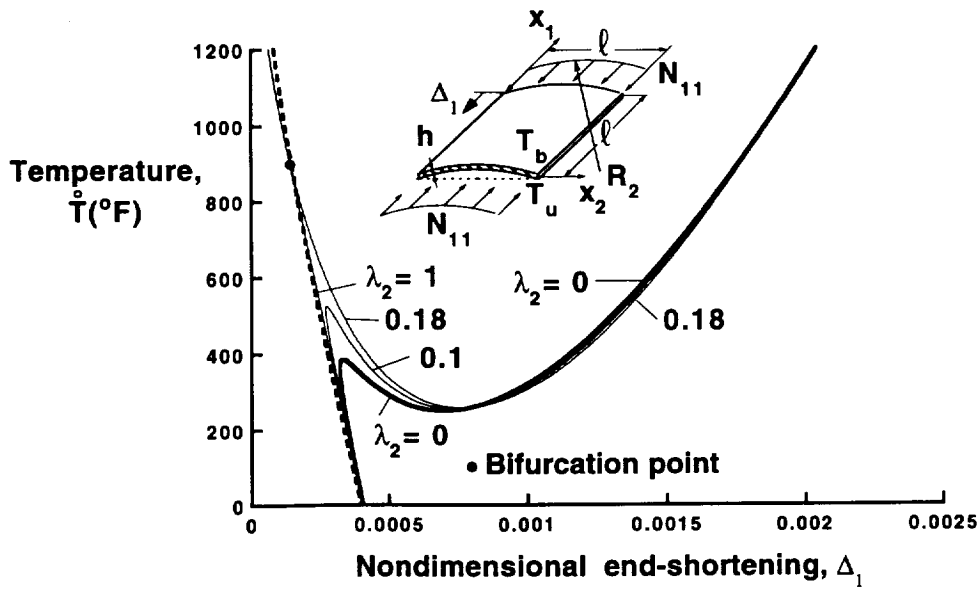

Fig. 12 Effects of tangentially restraining the straight edges on the postbuckling response of geometrically perfect cylindrical panels subjected to a through-the-thickness temperature gradient and a compressive edge load ($\ell / R_2 = 0.1$, $\tilde{L}_{11} = 0.75 (\tilde{L}_{11})_{cr}$).

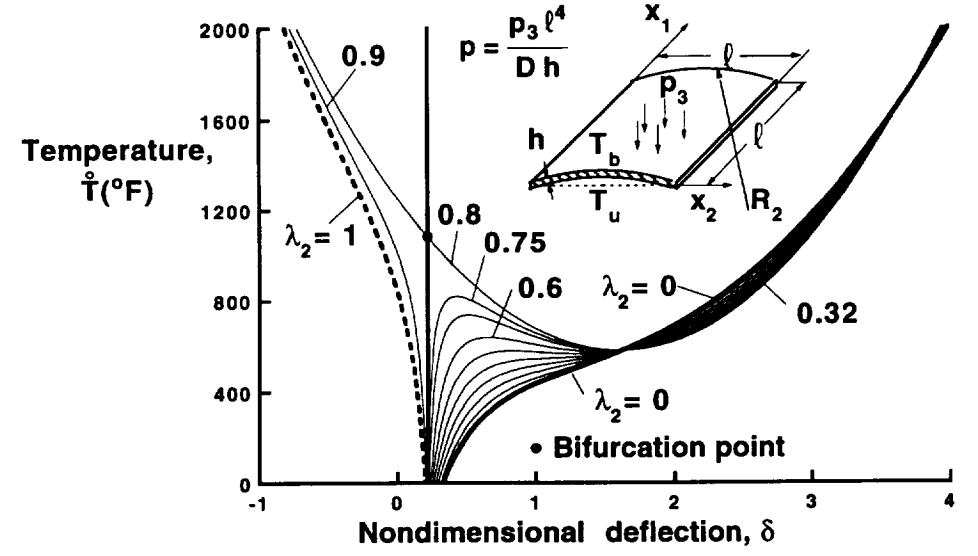

Fig. 13 Effects of tangentially restraining the straight edges on the postbuckling response of geometrically perfect cylindrical panels subjected to a through-the-thickness temperature gradient and a transverse pressure load ($\ell / R_2 = 0.1$, p = 2).